JOURNAL OF GEOPHYSICAL RESEARCH, VOL. 111, C06024, doi:10.1029/2005JC003101, 2006

Click Here for Full Article

CO_2 fluxes in the subtropical and subarctic North Atlantic based on measurements from a volunteer observing ship

Heike Lüger,[1] Rik Wanninkhof,[2] Douglas W. R. Wallace,[3] and Arne Körtzinger[3]

Received 14 June 2005; revised 20 January 2006; accepted 7 March 2006; published 17 June 2006.

[1] Surface seawater pCO_2 and related parameters were measured at high frequency onboard the volunteer observing ship M/V *Falstaff* in the North Atlantic Ocean between 36° and 52°N. Over 90,000 data points were used to produce monthly CO_2 fluxes for 2002/2003. The air-sea CO_2 fluxes calculated by two different averaging schemes were compared. The first approach used gas transfer velocity determined from wind speed retrieved at the location of the ship and called colocated winds, while for the second approach a monthly averaged gas transfer velocity was calculated from the wind for each grid pixel including the variability in wind. The colocated wind speeds determined during the time of passage do not capture the monthly wind speed variability of the grid resulting in fluxes that were 47% lower than fluxes using the monthly averaged wind products. The *Falstaff* CO_2 fluxes were in good agreement with a climatology using averaged winds. Over the entire region they differed by 2–5%, depending on the time-dependent correction scheme to account for the atmospheric in increase in pCO_2. However, locally the flux differences between the ship measurements and the climatology were greater, especially in regions north of 45°N, like the eastern sector. A comparison of two wind speed products showed that the annual CO_2 sink is 4% less when using 6 hourly NCEP/NCAR wind speeds compared to the QuikSCAT wind speed data.

Citation: Lüger, H., R. Wanninkhof, D. W. R. Wallace, and A. Körtzinger (2006), CO_2 fluxes in the subtropical and subarctic North Atlantic based on measurements from a volunteer observing ship, *J. Geophys. Res.*, *111*, C06024, doi:10.1029/2005JC003101.

1. Introduction

[2] The midlatitude North Atlantic acts as a major sink for atmospheric CO_2 throughout most of the year [*Lefèvre et al.*, 1999; *Takahashi et al.*, 2002], because of the cooling of surface waters and high biological productivity in this area. Warm salty water masses flow northeastward where the water cools and sinks due to increased density [*Dickson et al.*, 1996]. High biological productivity drives a considerable spring/summer CO_2 drawdown that counteracts the effect of seasonal warming on the saturation state of surface waters [*Takahashi et al.*, 2002]. In the North Atlantic Ocean the overall seasonal trend of CO_2 fluxes is quite well known, but uncertainty remains as to the magnitude and temporal variability. The surface ocean carbon cycle is highly dynamic which causes seawater partial pressure of CO_2 (pCO_2 sw) to vary seasonally up to 60% around the atmospheric pCO_2 level [*Takahashi et al.*, 2002]. Therefore high-frequency CO_2 measurements in the open oceans are required to characterize the oceanic carbon cycle. Moreover, there are several major sources of uncertainty for the determination of CO_2 fluxes including the well-known uncertainty associated with the gas exchange coefficient parameterization as a function of wind speed and the wind speed itself. In this paper, a seasonally resolved data set is used to quantify the monthly CO_2 fluxes and determine the effect of various error sources in CO_2 flux calculations with focus on the wind speed product.

[3] The EU-funded project CAVASSOO (Carbon Variability Studies by Ships Of Opportunity) initialized an Atlantic network of volunteer observing ships (VOS) to monitor seawater pCO_2 and related parameters. The VOS line data used here were collected on the Swedish car carrier M/V *Falstaff* which sailed year-round between Europe and the East Coast of the United States on a roundtrip of typically six weeks duration. From 2002 to early 2003, the M/V *Falstaff* crossed the North Atlantic 15 times and yielded on average 6000 pCO_2 sw data points per cruise with a spatial resolution of about 500 m (Figure 1). No wind speed was recorded onboard the ship, but wind speed data retrieved from satellite observations (QuikSCAT product) were colocated in time and space with pCO_2 and ancillary data to determine the flux. This high-density data set enables us to determine the effect of variability of ΔpCO_2 and wind speed within defined grid boxes and to estimate extrapolation errors. A previous publication [*Lüger et al.*, 2004] dealt with the seasonal variability of the surface $pCO_{2\ sw}$ of this data set and determined the factors controlling this parameter. This work looks at CO_2 flux calculation methods using the *Falstaff* data set. The focus is on

[1] Cooperative Institute of Marine and Atmospheric Sciences, Miami, Florida, USA.
[2] Ocean Chemistry Division, Atlantic Oceanographic and Meteorological Laboratory, NOAA, Miami, Florida, USA.
[3] Leibniz-Institut für Meereswissenschaften and der Universität Kiel (IFM-GEOMAR), Kiel, Germany.

Copyright 2006 by the American Geophysical Union.
0148-0227/06/2005JC003101$09.00

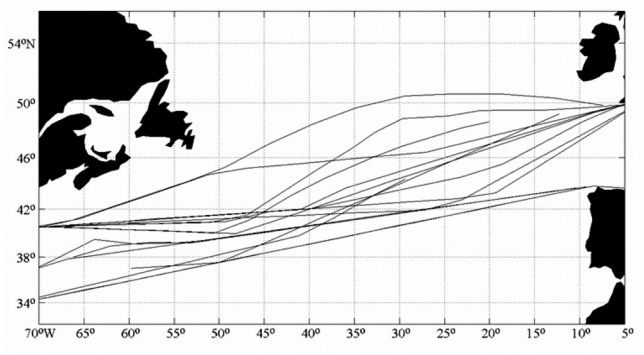

Figure 1. *Falstaff* cruises between Europe and the East Coast of the United States from February 2002 to January 2003. During these cruises, measurements of pCO_2 in seawater and air, temperature, and salinity were carried out. Wind speed data from QuikSCAT observations were colocated for each cruise.

averaging methods and the effect of possible cross correlation between ΔpCO_2 and wind speed. These are two aspects of CO_2 flux calculations that are poorly constrained in previous analyses that utilized sparser data. We also discuss the seasonal cycle of the CO_2 flux and compare our regional fluxes with those calculated using the global pCO_2 sw climatology of *Takahashi et al.* [2002]. Furthermore, we address the effect of different wind speed data sources on regional CO_2 flux estimates. A flux calculation scheme is proposed which will improve and reduce the error on current CO_2 flux estimates.

2. Methods

2.1. Data Collection and Analytical Methods

[4] In early 2002, the car carrier M/V *Falstaff* was equipped with an autonomous pCO_2 measurement system. The data from the first year of almost continuous operation of the VOS line is presented here. In addition to measurements of seawater pCO_2, temperature, and salinity at 1 min intervals, the mole fraction of atmospheric CO_2 in dry air (xCO_2) was measured every two hours. The CO_2 system was installed on the starboard side of the lowest deck in the engine room of the *Falstaff*. The seawater flowed into the system by hydrostatic pressure at a rate of about 15 l min^{-1}. This type of static water intake avoids bubble formation due to pump suction and cavitation processes which might bias the CO_2 measurement. The temperature of the seawater was measured at three locations: in situ at the seawater inlet (remote temperature sensor model 38, Seacat from Seabird Electronics Inc., Seattle, Washington), upstream of the equilibrator (thermosalinograph model 21, Seacat from Seabird Electronics Inc., Seattle, Washington), and within the equilibrator (Pt-100 temperature probe). The seawater flowed into the equilibrator where thermodynamic equilibrium is established with a nonrecirculating counter current flow of ambient air which flows at a rate of 150–200 mL min^{-1}. The tandem type equilibrator (Japanese patent P2001-83053A) was designed by Y. Nojiri and Kimoto Inc. (Tsukuba, Japan). It consists of two stages: a bubbling equilibrator and static mixing equilibrator with a reported overall equilibration efficiency of 99.5%. The efficiency is defined as the percentage of an initial air-water pCO_2 disequilibrium that is removed during the one-way passage of the sample air through the tandem equilibrator. The equilibrated air is pumped into the measurement unit where it is dried in several steps [*Lüger et al.*, 2004]. After drying, the sample gas enters a nondispersive infrared detector unit (model 6252, LICOR, Inc., Lincoln, Nebraska). The equilibrated air is calibrated against three calibration gases (working standards) with a nominal range of 250 to 450 ppmv. The three standard gases were provided by Deuste & Steininger GmbH (Mühlhausen, Germany). The working standard gases were calibrated against standard gases provided by the Climate Monitoring and Diagnostics Laboratory of NOAA, Boulder, Colorado (now Global Monitoring Division of the Earth System Research Laboratory (ESRL)) of similar concentration range using an NDIR analyzer (LICOR model 6262). This procedure yielded an accuracy of 0.07 ppmv for our working standards relative to the NOAA values.

[5] The CO_2 concentration was calculated from the NDIR voltage signal and the voltage was corrected for atmospheric pressure as well as temperature changes within the NDIR optical cell. The corrected voltage readings were converted into CO_2 (dry) mixing ratios (xCO_2) using a least squares procedure for the quadratic regression function calculated from the calibration standards, excluding the zero gas. The pCO_2 sw was calculated from the xCO_2 at 100% humidity and corrected to in situ temperature obtained from the remote sensor at the seawater intake assuming $\delta pCO_{2sw}/\delta SST = 4.23\%/°C$ [*Takahashi et al.*, 1993]. The temperature deviation between the equilibrator and the in situ temperature was very small, ranging typically between 0.01 and 0.03°C. This temperature increase is substantially less than the 0.2 to 0.3°C observed on other systems [*Feely et al.*, 1998].

[6] Atmospheric CO_2 measurements were obtained every 2 hours and the atmospheric pCO_2 values were calculated similar to the seawater pCO_2 routine except that no temperature correction was applied. Monthly averages of the atmospheric data of all cruises were compared to monthly averages of flask measurements available from the NOAA/ESRL flask network (http://cmdl.noaa.gov) at four different locations: Azores, Ireland, Iceland, and Bermuda. The flask data of the four sites were combined to monthly averages. The *Falstaff* xCO_2 values were slightly higher than the monthly flask measurements during the 12 months of observations with a difference of 0.72 ± 1.0 ppmv (Figure 2).

2.2. Air-Sea Flux Calculation Schemes

[7] Regional air-sea fluxes of CO_2 are commonly determined from the product of the sea-air partial pressure difference, ΔpCO_2, gas transfer velocity, k, that is parameterized with wind speed and solubility of CO_2 in water, K_0, which is mainly controlled by temperature:

$$F = (pCO_2\ sw - pCO_2\ atm)k\ K_0 = \Delta pCO_2\ k\ K_0 \qquad (1)$$

The measurements of seawater and atmospheric pCO_2, sea surface temperature (SST), and sea surface salinity (SSS) from the M/V *Falstaff* were collected between 2002 and

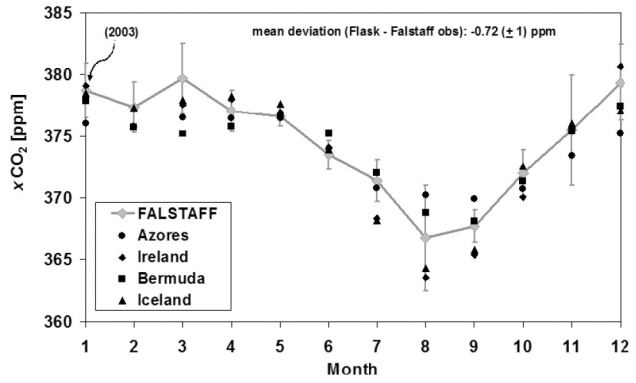

Figure 2. Comparison between atmospheric xCO_2 measurements in 2002 from *Falstaff* observations and measurements from the NOAA/CMDL flask network, respectively. The 2003 January flask data were corrected by adding 1.6 ppm to the 2002 value since at that time, no results were available. The averaged flask measurements for each location were 0.72 (±1) ppm lower than the *Falstaff* results.

2003. Since no wind speed measurements were taken onboard the *Falstaff*, we used colocated QuikSCAT winds. Each individual cruise was combined with QuikSCAT satellite wind speed data using all data within 25 km and 5 hours of the pCO_2 sw observations. We used the level 2B QuikSCAT wind speed product with a resolution of 25 km retrieved from NASA's Seawinds Scatterometer representing wind speed at 10 m height. The data was obtained from the Physical Oceanography Distributed Active Archive Center of JPL at http://podaac.jpl.nasa.gov. QuikSCAT data that were flagged as contaminated by rainfall was not used. Overall there were colocated QuikSCAT winds for 48% of all cruise data.

[8] Two issues, in particular, require careful attention when calculating air-sea gas fluxes. Some of the input parameters are averaged quantities, and when they are multiplied the covariance of the properties must be taken into account. Also, the relationship between gas transfer velocity and wind speed used is nonlinear, and the results are dependent on the variability of the wind over the averaging interval. The relationship of gas transfer and wind proposed by *Wanninkhof* [1992, hereinafter referred to as W92] is used here:

$$k = 0.31\ U^2(Sc/660)^{-1/2} \tag{2}$$

Where k is in cm hr^{-1}, U is the wind speed in m s^{-1} referenced to 10 m, and Sc is the Schmidt number provided as a function with temperature. The time-averaged gas transfer velocity k_{av} can be written as:

$$k_{av} = 0.31\ U_{av}^2\left(\left(\Sigma U^2/n\right)/\left(U_{av}\right)^2\right)(Sc/660)^{-1/2} \tag{3}$$

where $((\Sigma U^2/n)$ is the second moment, the variance of the wind speed, and $((\Sigma U^2/n)/(U_{av})^2)$ is referred to as the nonlinearity factor, R. More detail on the statistical background of R, is given by *Wanninkhof et al.* [2002]. In W92 it is assumed that the distribution of winds around its mean follows as Rayleigh distribution which yields an R of 1.26. Therefore their k_{av} expression is: $k_{av} = 1.26\ 0.31\ U_{av}^2 (Sc/660)^{-1/2} = 0.39\ U_{av}^2 (Sc/660)^{-1/2}$. Here, we utilize a comprehensive data set to look at the effect of averaging the wind. Because of the high temporal resolution of QuikSCAT wind products, R can be determined for the appropriate averaging interval yielding a more accurate result than using the Rayleigh wind distribution as done in W92.

[9] The flux calculation requires knowledge of seawater pCO_2 (pCO_2 sw), atmospheric pCO_2 (pCO_2 atm), SST, and wind speed. Since pCO_2 atm was measured every two hours in between the seawater measurements, the values were interpolated to match the seawater pCO_2. The colocated QuikSCAT wind speed data had to be interpolated when data gaps occurred at times when there was no satellite coverage. Both pCO_2 atm and colocated QuikSCAT winds were linearly interpolated using a time-weighted interpolation scheme. The equation was:

$$x_t = \left(x_{pre} * \left(t_{post} - t\right) + x_{post} * \left(t - t_{pre}\right)\right)/\left(t_{post} - t_{pre}\right) \tag{4}$$

where x_t is the parameter value, i.e., atmospheric pCO_2 or wind speed, at the time the pCO_2 data point was taken (t), x_{pre} and x_{post} are the measured parameter values prior to and after the time of interpolation, and (t_{pre}) and (t_{post}) refer to the times of the measurements prior to and after the time of interpolation. Using this approach all seawater pCO_2 measurements were matched with an atmospheric pCO_2 and a wind speed value.

[10] The monthly CO_2 air-sea fluxes for a 4° latitudinal by 5° longitudinal grid were determined using two different approaches.

[11] 1. By calculating the monthly CO_2 fluxes from the cruise data within each grid box for the particular month using the 1 min pCO_2 sw values, pCO_2 air values and the colocated QuikSCAT winds ($F_{1\text{-min avg}}$). The resulting 1 min fluxes were then averaged for the appropriate 4° × 5° grid for each month. It is assumed that the average of the 1 min fluxes obtained during 9–12 hour passage across a grid box is representative for the grid box.

[12] 2. Using monthly 4° × 5° averaged values of ΔpCO_2, K_0 and k to calculate the CO_2 flux. This is the approach which is most commonly used. However, in this work we account for the variability in k over the grid box for the appropriate month by multiplying the averaged k with the nonlinearity factor, R. The flux is calculated for each grid square per month and referred to as $F_{grid\ avg}$. The gas transfer velocity k in this approach is calculated from QuikSCAT winds retrieved for the entire box, not just along the cruise track as in the approach 1. Per 4° × 5° grid box there are on average over 14,000 QuikSCAT satellite observations per month. This is a much higher yield than the cruise colocated QuikSCAT winds which amount on average to approximately 400 satellite observations during a particular transect across a grid box per month.

[13] The following equations describe the two approaches:

$$F_{1\text{-min avg}} = \overline{k_{1\,min\ avg} K0 \Delta pCO_2} \tag{5}$$

$$\begin{aligned} F_{grid\,avg} = R\ & \overline{k}_{gridavg}\ \overline{K_0}\ \overline{\Delta pCO_2} + \overline{K_0}\ \overline{k'\Delta pCO_2'} \\ & + \overline{k}_{gridavg}\ \overline{K_0'\Delta pCO_2'} + \overline{\Delta pCO_2}\ \overline{K0' k}_{gridavg} \\ & + \overline{K_0' k' \Delta pCO_2'} \end{aligned} \tag{6}$$

where $k_{1\text{min }avg}/k_{gridavg}$ is the transfer velocity, K_0 is the solubility coefficient of CO_2, and ΔpCO_2 is the sea-air gradient of CO_2 partial pressure (pCO_2 sw $-$ pCO_2 atm). R is the nonlinearity factor, which is determined from all QuikSCAT wind speed observations in the 4° × 5° grid over a monthly timescale (=averaged winds), and the prime indicates the variance around the mean. The overbar indicates averaged values of each month and each 4° × 5° grid. The solubility of CO_2 (K_0) and the Schmidt number were computed by the equations of *Weiss* [1974] and *Wanninkhof* [1992], respectively, and using the monthly 4° × 5° SST average. The transfer velocity k was calculated using the respective QuikSCAT product and the parameterization for short-term winds of W92. In equation (5) we use QuikSCAT winds that were colocated with the cruise data and calculate $k_{1\text{min }avg}$, whereas in equation (6) we use QuikSCAT winds retrieved for the entire grid and month to calculate $k_{gridavg}$.

[14] The covariance terms are estimated taking advantage of the high density of measurements. Therefore the spatial and temporal variability in the flux calculations is accounted for with respect to wind speed variability. We are assuming that the spatial variability in pCO_2 sw in each box for each month is represented by the variability of pCO_2 sw along the cruise track during passage across a particular box for a given month.

[15] The covariance terms in equation (6) acknowledge any deviation from averaged values on a submonthly scale, and they were calculated following the approaches by *Olsen et al.* [2004] and *Keeling et al.* [1998].

[16] To estimate the effect of different wind products on the flux results, 6 hourly NCEP/NCAR Reanalysis wind speed data were compared to the QuikSCAT product. The NCEP/NCAR Reanalysis winds were retrieved from the NOAA-CIRES Climate Diagnostics Center, Boulder, Colorado (http://www.cdc.noaa.gov/). Note, that these data were monthly averages of the 6 hour surface flux products for each 4° × 5° grid, and they are referenced to 10 m, as were the QuikSCAT wind data.

[17] The fluxes calculated with the *Falstaff* data were compared to fluxes for the same 4° × 5° grid boxes using the ΔpCO_2 climatology of *Takahashi et al.* [2002] (http://www.ldeo.columbia.edu/res/pi/CO2/carbondioxide/air_sea_flux/). Since this climatology refers to conditions of the nominal year 1995, the ΔpCO_2 data must be corrected for the temporal increase in anthropogenic CO_2. Two approaches were pursued.

[18] 1. All of the climatological ΔpCO_2 data except for the data north of 45°N were assumed to represent the year 2002. That is, the surface ocean CO_2 levels south of 45°N keep up with the atmospheric increases and the ΔpCO_2 remains invariant over time. The climatological ΔpCO_2 data north of 45°N were increased by 1.6 μatm per year, which amounts to a total of (1.6 × 7=) 11.2 μatm. It is assumed that due to deep convective mixing at high latitude the surface water pCO_2 levels do not increase with time in response to an increasing atmospheric CO_2 level. This is the assumption that *Takahashi et al.* [2002] uses.

[19] 2. For the entire domain the surface water pCO_2 levels keep up with the atmospheric CO_2 increase and all climatological ΔpCO_2 data were taken as is.

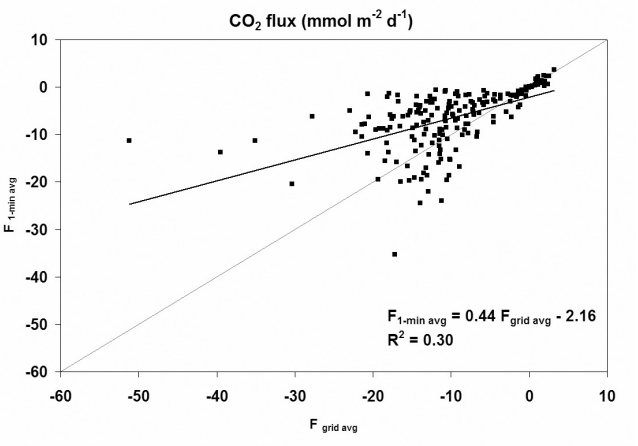

Figure 3. Comparison between two flux calculation schemes. The 1 min averaged fluxes ($F_{1\text{-min avg}}$) were calculated from the cruise data points and colocated QuikSCAT winds and subsequently averaged to a 4° × 5° grid, whereas the grid-averaged fluxes ($F_{\text{grid avg}}$) were calculated from the monthly 4° × 5° averages of the ΔpCO_2 and QuikSCAT winds retrieved from the entire grid. The black line shows the linear, and the gray line shows the 1:1 trend line. For the detailed flux calculation please refer to the method section.

[20] The CO_2 fluxes are calculated using the same scheme as listed above employing QuikSCAT winds (4° × 5° monthly averages), W92 parameterization and the correction for the nonlinearity factor R (equation (6)). The covariance terms, however, are not included, since the cruise data from which the average climatological values are derived are not available.

3. Results and Discussion

3.1. Extrapolation Procedures

[21] Calculation of CO_2 fluxes for a given grid box from wind speed observations that are made along with pCO_2 sw observations, e.g., employing shipboard winds, does not take into account the wind speed variability that occurs within the entire grid box. Here we show that the use of shipboard winds, which we simulate by using colocated QuikSCAT data, can indeed introduce significant deviations in the flux results when extrapolated over a larger region. The effect of the two different averaging schemes on the CO_2 flux is shown in Figure 3 and the difference between the two approaches is considerable. The 1 min flux averages ($F_{1\text{-min avg}}$) using colocated winds are 47% lower, i.e., suggest a smaller CO_2 sink, than the grid-averaged fluxes ($F_{\text{grid avg}}$). This flux bias arises primarily as a result of the different wind speed variability represented in the colocated and averaged winds. Because of the nonlinearity of k as a function of wind speed, the effects of averaging are greatest for grid boxes and months with very strong wind speed variability. In September 2002 (48°N, 47.5°W), for instance, the flux bias was large ($F_{\text{grid avg}} - F_{1\text{-min}} = (-20.7) - (-1.4) = -19.3$ mmol m^{-2} d^{-1}). This is directly associated with differences in variability in wind speed. The

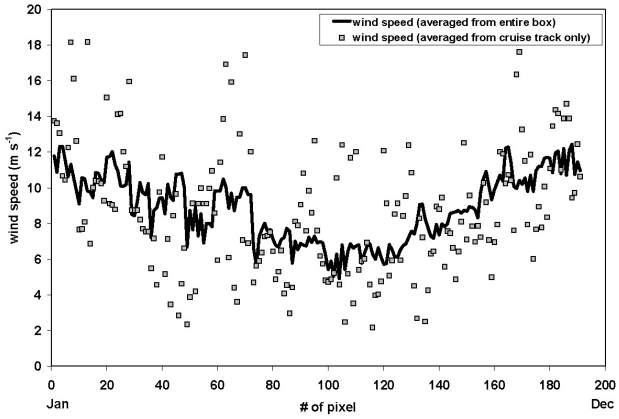

Figure 4. QuikSCAT wind speed data averaged for each 4° × 5° grid box and month using different averaging schemes. The grid-averaged data are based on satellite data points that were retrieved for each entire grid box (solid line). For the second set of wind speed data, only wind speed data were considered that were observed along the cruise track within each grid box and month (squares).

colocated wind speed data display a greater scatter than the grid-averaged wind speed data in this data set (Figure 4), but the grid averages are on average 0.2 m s^{-1} higher than the colocated wind speeds. Shipboard wind speed measurements, or in this case colocated QuikSCAT winds, do not capture the wind speed variability of an area much greater than the cruise track. Therefore wind speed products should be used that include these wind speed statistics and account for the spatial variability of the entire grid. Temporal wind speed changes during a single cruise, e.g., during their approximate 12 hour passage through a 4° × 5° grid, do not represent the wind speed variability of an entire month. It is more accurate to use the monthly wind speed variance (=2nd moment) in order to capture not only the spatial but also the temporal wind speed variability.

[22] The seawater pCO_2 usually changes less rapidly compared to the wind speed, and therefore it is reasonable to extrapolate cruise data to the entire grid and month. *Sweeney et al.* [2002] showed that the decorrelation length scales for pCO_2 sw are on the order of 500–1500 km such that extrapolation and averaging of the pCO_2 sw over the grid should not introduce large errors especially if the covariance terms are taken into account. Here, we consider grid boxes of 4° latitudinal and 5° longitudinal extend which is less than decorrelation length scales, and therefore it is assumed that the pCO_2 sw along the track are representative for the entire grid box. The temporal extrapolation from cruise data to monthly averages probably does not introduce large errors, either, since the equilibration time of surface seawater for pCO_2 with respect to air-sea gas exchange is rather slow (~1 year) due to the chemical reactions of the carbonate system in seawater. A notable exception will be during periods of biological blooms when CO_2 drawdown can be large over periods of weeks [*Chipman et al.*, 1993]. Use of pCO_2 sw algorithms retrieved from, for instance, SST, might be a more robust way to address variability within a pixel [*Olsen et al.*, 2004].

[23] We included covariance terms in the calculation of the grid-averaged fluxes. These terms account for any cross correlation between the ΔpCO_2, transfer velocity, or solubility on submonthly scales. In our data set the effect of the covariance terms decreased the flux on average by 1% annually for the entire area with an average deviation of 0.1 mmol m^{-2} d^{-1} (Figure 5). In a model approach *Keeling et al.* [1998] calculated an effect between 0 and 4% for the covariance effect for O_2 in the subtropical gyre of the North Atlantic, which is within the range of our calculation. Mostly the covariance terms in the *Falstaff* data set were negative, thus increasing the oceanic CO_2 sink when applied. We found that only the first covariance term of equation (6), $\overline{K_0 k' \Delta pCO_2'}$, significantly changed the CO_2 flux whereas the effect of the latter three terms were negligible. The first covariance term amounted to on average 6% of the flux value. *Olsen et al.* [2004] report that the covariance terms ranged between −0.2 and 0.4 mmol m^{-2} d^{-1} when considering a global data set. However, they also state that the variability of the QuikSCAT wind data set used was low which directly effected the covariance terms. When they doubled the variation for the wind speed their covariance terms increased significantly to about 5–15 mmol m^{-2} d^{-1}. Our covariance terms ranged between a maximum and minimum of 2 and −2 mmol m^{-2} d^{-1}, respectively. It is mainly the wind speed variability which changes the covariance terms, because it displays the greatest short-term variability. Effects of ΔpCO_2 and/or temperature changes on the cross correlation are only significant when steep gradients occur which is illustrated in the following case study.

[24] For the pixel centered at 57.5°W, 44°N in December 2002 we observe larger changes in ΔpCO_2 and solubility than other pixels (Figure 6). The average colocated wind speed for this grid was 11 ± 5 m s^{-1} and the variance (=2nd moment) was 21 m^2 s^{-2} when estimated from QuikSCAT data during December. In this grid box we find a ΔpCO_2 range of about 150 μatm corresponding to a pronounced

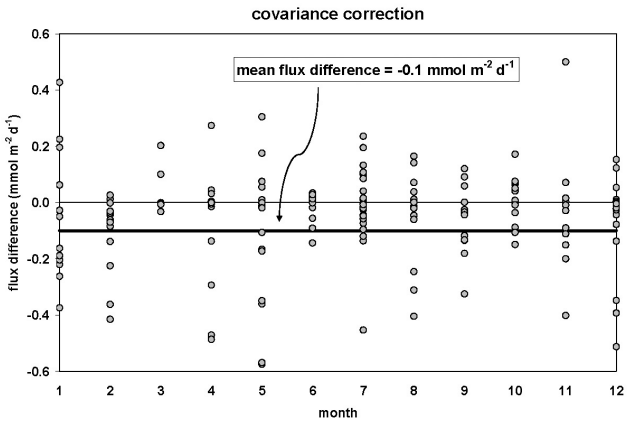

Figure 5. Effect of the covariance terms on the flux calculation. The monthly difference between fluxes based on a 4° × 5° resolution with and without the covariance terms from equation (6) is shown. Only the data within the ±1 s limits are shown. The mean flux difference shows that the uncorrected fluxes are 0.1 mmol m^{-2} d^{-1} lower than the fluxes corrected for the covariance terms.

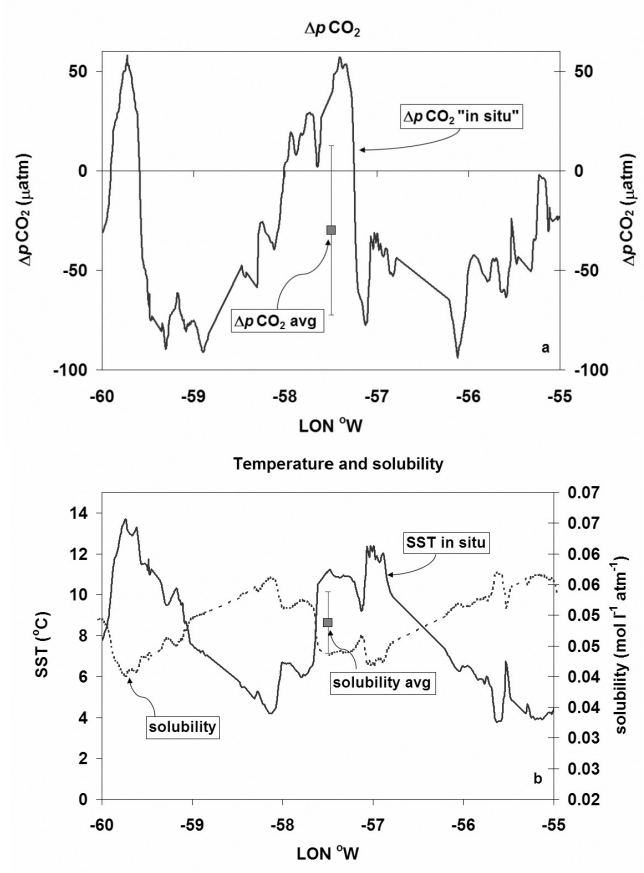

Figure 6. Example of short-term variability of ΔpCO_2, solubility, and SST for the grid box 57.5°W, 44°N for the December cruise in 2002. The continuous gray lines represent the observed (a) ΔpCO_2 and (b) SST data. The solubility data are represented by the dotted gray line (Figure 6b). The squares are the averages of the grid box: ΔpCO_2 (Figure 6a) and solubility and SST (Figure 6b).

SST gradient of about 10°C. This change occurred within 15 hours and is explained by crossing a front along the cruise track. Aside from a large SST increase, the salinity increased from 31.96 to 34.78. The CO_2 flux including the covariance terms was about 10% higher when compared to the noncorrected flux which increased from 28 to 30 mmol m^{-2} d^{-1}. This example illustrates that especially in regions of diverse ocean surface currents extrapolation of CO_2 fluxes from direct observations can lead to bias if low observation density is available. This can be circumvented by robust algorithms which can be created between pCO_2 sw and parameter that are measured at higher frequency. The averaged fluxes ($F_{grid\ avg}$) calculated from equation (6) will be used in all following calculations, because these include a better representation of the wind speed for the grid boxes.

3.2. Regional Flux Patterns

[25] Generally, the source-sink CO_2 flux pattern is driven by counteracting and seasonally dependent effects: thermodynamics, biology and air-sea gas exchange. The isochemical thermal effect on seawater pCO_2 is 4.23% $°C^{-1}$ [*Takahashi et al.*, 1993] and yields a 14 μatm increase of pCO_2 per degree temperature increase for seawater at 330 μatm. Summer warming will therefore significantly increase the pCO_2 sw. Net biological production decreases pCO_2 sw values and leads to increased CO_2 uptake by the ocean, particularly during spring time. Because of their synchronicity, the spring time warming and the spring phytoplankton bloom have counteracting effects on the pCO_2 sw. In the wintertime cooling and higher winds prevail. Because of the quadratic nature of the gas exchange–wind speed relationship high winds will greatly increase the magnitude of the CO_2 sink.

[26] Monthly flux maps covering an annual cycle of the CO_2 flux in the mid latitude North Atlantic for 2002 are shown in Figure 7. The contour plots show variable monthly coverage which depends on the ship routes for the particular month. Aside from natural variability this will affect month-to-month flux variations as well. The observed area is a sink for CO_2 except in restricted regions during summer. The fluxes are close to neutral with slight outgassing in the summer and increased CO_2 uptake during winter. The CO_2 fluxes range from +3 to −51 mmol m^{-2} d^{-1} in July (40°N, 52.5°W) and December (40°N, 62.5°W), respectively. During summertime, the thermodynamic forcing on the CO_2 flux is dominant leading to outgassing, especially in the western region. In the wintertime both cooler temperatures and higher winds increase the CO_2 sink.

[27] The eastern (10°–35°W) and the western (36°–70°W) sectors of the cruise tracks show different flux patterns. The majority of samples taken in the eastern sector are at the same time more northerly than samples taken in the western sector. The most noticeable CO_2 flux difference between the sectors occurs in summertime, when the fluxes in the two sectors have different signs (Figure 8). Slight CO_2 outgassing occurs in July and August mainly in the western sector. The effect of summer warming is more apparent in the western sector than in the eastern sector [*Lüger et al.*, 2004]. Here the seawater temperature is on average 4°C higher than in the eastern sector from June to September. This temperature difference affects the seawater pCO_2 and makes the western sector a slight source for CO_2 during the July and August. The differences in the ΔpCO_2 between the eastern (−21 μatm) and the western (+6 μatm) sector during this time are pronounced, whereas the transfer velocities are the same in the two sectors (3 cm hr^{-1}). It is thus the ΔpCO_2 value rather than the transfer velocity that causes the differences in fluxes between the two in July and August. In December, on the other hand, the flux bias is caused not only by a significant difference in ΔpCO_2 (east: −23 μatm, west: −34 μatm), but also by a greater difference in transfer velocity (east: 11 cm hr^{-1}, west: 13 cm hr^{-1}). The wintertime carbon uptake from December to February in the western sector is higher (−18 mmol m^{-2} d^{-1}) than in the eastern sector (−12 mmol m^{-2} d^{-1}).

[28] The flux differences between the western and eastern sectors likely reflect characteristics of the subtropical and subpolar gyres. The *Falstaff* lines did not cover the entirety of either gyre but rather sampled at the margins of both, as well as at the boundary between them. The transfer velocities were on average higher in the eastern sector due to higher wind speeds, whereas a larger ΔpCO_2 was observed in the western sector. In the eastern sector the annual carbon

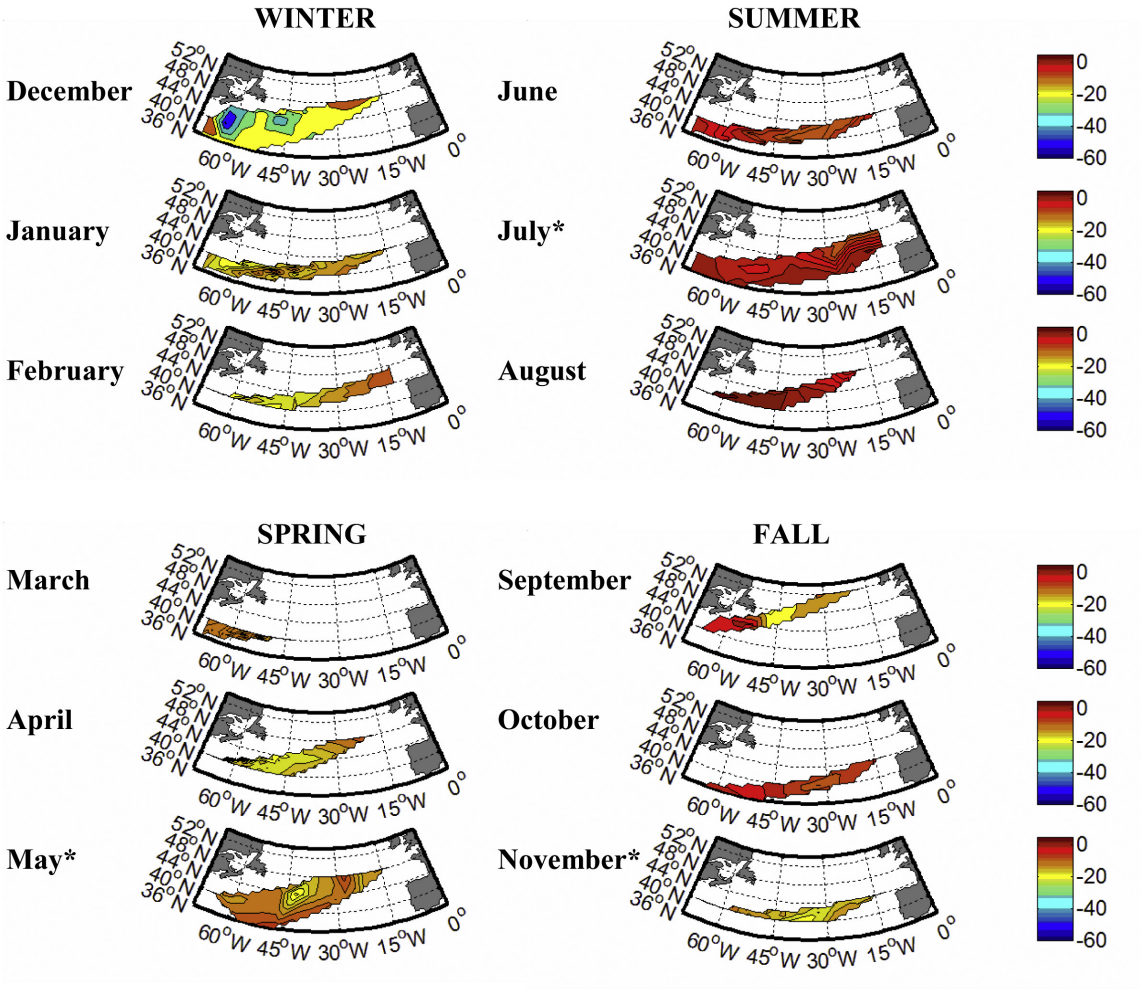

Figure 7. Contour maps of CO_2 fluxes calculated from *Falstaff* data that were averaged to a 4° × 5° grid for all cruises ($F_{grid\ avg}$). For detailed calculation and gridding procedure, please refer to section 2. Asterisk indicates two cruises were used for the flux calculation in some months.

sink was 46% less ($F_{grid\ avg} = -18$ Tg C yr^{-1}, area: 7×10^6 km^2) compared to the western sector ($F_{grid\ avg} = -33$ Tg C yr^{-1}, area: 10×10^6 km^2).

3.3. Effect of Wind Speed Products on the CO_2 Flux

[29] A major source of uncertainty for the calculation of CO_2 flux is the choice of wind speed products. Significant improvements to global wind speed data include the use of assimilation products and remotely sensed data. Since the air-sea flux is strongly wind speed dependent, it is crucial to use wind products that are accurate and of high density. We analyze the sensitivity of the CO_2 flux to the wind speed product by comparing the fluxes calculated from satellite data (QuikSCAT) with those calculated reanalysis data (NCEP/NCAR). Both flux estimates were calculated following the approach described in section 2.2. The QuikSCAT data products are based on the 4° × 5° monthly resolution and referenced to a height of 10 m. The NCEP/NCAR data are retrieved from 6 hourly surface flux products referenced to a height of 10 m and are in a nonregular (Gaussian) grid. The Gaussian grid had an approximate 2° × 2° resolution and the data were averaged to the 4° × 5° monthly resolution.

[30] The annual CO_2 sink was reduced by 4% when using 6 hourly NCEP/NCAR wind speeds (−48.4 Tg C yr^{-1}) compared to fluxes calculated with QuikSCAT wind speed data (−50.5 Tg C yr^{-1}; Table 1). Only in February and in September, the NCEP winds were slightly greater than the QuikSCAT winds, but the difference was small. The maximal bias on a monthly scale occurred in August (0.54 m s^{-1}). The wind speed difference was slightly higher in the western sector (0.3 m s^{-1}) than in the eastern sector (0.1 m s^{-1}) with NCEP winds always being lower than QuikSCAT winds.

[31] It was expected that the NCEP/NCAR reanalysis data yielded a smaller CO_2 sink than the satellite derived QuickSCAT wind speed data. Generally, it is assumed that the satellite data display higher variability by capturing the small-scale and high-wind events better than the reanalysis products [*Doney*, 1996; *Wanninkhof et al.*, 2002].

[32] The bias between wind speed data will certainly depend on the geographic region and season. It has been

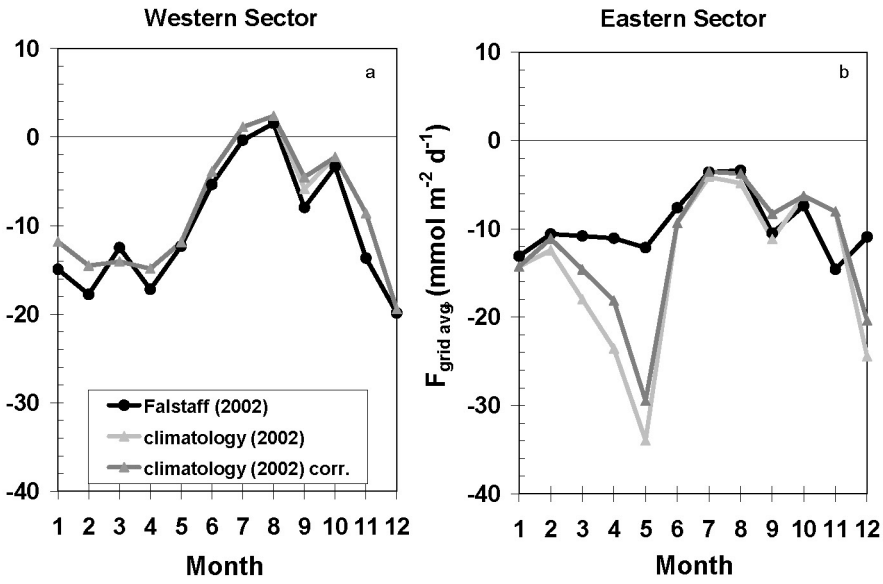

Figure 8. Monthly averages of the CO_2 flux, $F_{grid\ avg}$, for the *Falstaff* data set (light gray dots) and the Takahashi et al. climatology (black and gray triangles) in the (a) western and (b) eastern sector. Two CO_2 flux results are shown: (1) using ΔpCO_2 data from the climatology that were used as is and not corrected for an annual pCO_2 increase of 1.6 μatm at locations north of 45°N (black triangles) and (2) using ΔpCO_2 with the corrections applied as suggested by *Takahashi et al.* [2002] (gray triangles). Both data sets were combined with the same wind speed product (QuikSCAT, averaged for the entire grid box/month) and wind speed parameterization (W92). No data were collected in the eastern sector and in March.

discussed that satellite measurements of wind speed, e.g., SSM/I (Special Sensor Microwave Imager), deviate from reanalysis products depending on time and space [*Meissner et al.*, 2001]. *Olsen et al.* [2005] showed that the transfer velocity calculated with the NCEP/NCAR winds was lower compared to QuikSCAT when considered globally. In the region around 50°N they observed that the transfer velocity determined by QuikSCAT was increased at most by 2 cm h^{-1} relative to the NCEP/NCAR result. In our data set we find a smaller bias in the same direction and calculate a 0.4 cm h^{-1} positive offset in transfer velocity for the NCEP/NCAR data compared to the QuikSCAT data.

[33] Using the nonlinearity factor (R) rather than the long-term parameterization (0.39) decreases the annual CO_2 flux result for the QuikSCAT and NCEP/NCAR data set by 8.3% and 7.7%, respectively. If the variance in the wind speed is available, it is recommended to include the nonlinearity factor in the flux calculation since it is statistically more robust. The nonlinearity factor R depicts the deviation of wind speeds from the steady wind scenario. Globally R is 1.14 ± 0.07 and steady winds retrieved from NCEP/NCAR result in an R factor of 1 [*Wanninkhof et al.*, 2002]. Both wind speed products deviate slightly from the global mean value and yield for the QuikSCAT and NCEP/NCAR result 1.17 and 1.18, respectively.

3.4. CO_2 Flux Comparison to Climatology

[34] The most common calculation procedures to determine regional and seasonal fluxes use pCO_2 data that have been averaged to a certain grid resolution. *Takahashi et al.* [2002], for instance, report pCO_2 data that had been averaged to a 4° × 5° grid. These data are often used in model approaches in order to calculate CO_2 fluxes. *Takahashi et al.* [2002] compiled a global surface pCO_2 climatology based on about 940,000 measurements. The *Falstaff* data set contains approximately 90,000 data points from the midlatitude North Atlantic alone. The data are binned into 39 cells of 4° × 5° grid between 36° and 52°N with nearly monthly

Table 1. Annual Fluxes Determined From the *Falstaff* and the Takahashi Data Sets in 2002 and for Different Wind Speed Sources (QuikSCAT and 6 hourly NCEP/NCAR Winds

		Falstaff $F_{grid\ avg}$ 2002		
	Falstaff $F_{1\text{-}min}$ 2002	QuikSCAT	NCEP/NCAR	Takahashi 2002[a]
Latitude	36–52°N	36–52°N	36–52°N	36–52°N
Longitude	10–70°W	10–70°W	10–70°W	10–70°W
Flux, Tg C yr^{-1} $area^{-1}$	−32.1	−50.5	−48.4	−53.2
Wind speed	QuikSCAT	QuikSCAT	NCEP/NCAR	QuikSCAT
Area, 10^6 km^2	17	17	17	17
Parameterization	W92	W92	W92	W92

[a]Not corrected north of 45°N is *Takahashi et al.*'s [2002] suggestion.

coverage per grid. Flux differences between these two data sets, calculated from equation (6), originate from differences in ΔpCO_2 and/or SST data and/or binning procedures. The same wind speed data and parameterization of the gas exchange coefficient were used for the flux calculations in both data sets.

[35] The comparison to the climatology by *Takahashi et al.* [2002] shows that the annual carbon sink for the Takahashi (-53.2 Tg C yr^{-1} $area^{-1}$) and the *Falstaff* data sets (-50.5 Tg C yr^{-1} $area^{-1}$) differ by only 5% when assuming that ΔpCO_2 increases over time at latitudes greater than 45°N, in the way recommended by *Takahashi et al.* [2002] (Table 1). The appropriateness of this assumption for the North Atlantic has been questioned as some indications are that the North Atlantic pCO_2 sw increases at a rate faster than that of the atmosphere and therefore the ΔpCO_2 might even decrease with time [*Wallace*, 2002; *Anderson and Olsen*, 2002; *Völker et al.*, 2002]. When all the climatological ΔpCO_2 data are corrected for a temporal pCO_2 increase, thus keeping the ΔpCO_2 invariant over time, the bias between the two data sets gets smaller (2%). In this case the predicted annual climatological sink is reduced to -49.4 Tg C yr^{-1} $area^{-1}$. This implies that the sink calculated with the *Falstaff* data is indistinguishable from the climatological data collected over a time span of 30 years.

[36] While the net flux determined from our data set and the climatology is similar, we nevertheless find significant differences in spatiotemporal patterns of the flux between the two data sets when the data sets are separated into eastern and western sectors. The *Falstaff* data set shows a 16% larger annual sink than the climatology in the western sector (Figure 8a). In the eastern sector the opposite effect is observed and the annual *Falstaff* uptake rates are 44% lower than the climatological uptake rates. The Takahashi climatological data predict a much larger CO_2 sink than the *Falstaff* data in this sector in May and December, with the 'climatological' May sink being twice as strong (Figure 8b). During these months the ΔpCO_2 difference for certain pixels between the two data sets is as large as 43 μatm (May) and 49 μatm (December). The differences in annual average fluxes can in part be attributed to the time-dependent correction of the pCO_2 sw. The data were corrected in order to account for the anthropogenic CO_2 increase in the atmosphere and surface waters. In the western sector the uncertainty associated with whether or not to apply this correction makes less difference, because fewer observations were made north of 45°N. In the eastern sector on the other hand the correction has a stronger influence. If, following *Takahashi et al.* [2002], no correction for the climatological pCO_2 sw increase north of 45°N is applied, then the annual average flux difference in the western and eastern sector is, as stated above, 16% and 44%, respectively. However, if the climatological pCO_2 sw data that are located north of 45°N follow the atmospheric CO_2 increase, then the average flux bias between the two data sets stays nearly the same for the western sector (17%), but is significantly smaller in the eastern sector (25%) since here more grids were located north of 45°N. Clearly, the question if pCO_2 sw is changing is a significant issue for the estimation of contemporary fluxes at high latitudes and potentially also in upwelling regions based on historical data. The differences between the climatology and the *Falstaff* data set can also be caused by interannual variations of the surface pCO_2 sw. The season 2002/2003 might have been a year where this parameter displayed a different variability compared to the climatology.

[37] This comparison illustrates one of the problems associated with extrapolating air-sea CO_2 fluxes from one decade to another. Resolution of this issue will require continued collection of sea surface pCO_2 data on sector scales as well as a better understanding of the relationship between air-sea flux, carbon transport convergence and deep mixing within ocean sectors.

4. Summary

[38] The air-sea CO_2 flux is commonly estimated from indirect methods based on sparse estimates of the pCO_2 gradient between the seawater and the overlying atmosphere, the wind speed and the CO_2 solubility. The relatively large amount of data collected during 1 year of *Falstaff* operations shows that the continued employment of VOS can greatly improve data coverage and offer insights on the effect of variability on the flux calculations. The main findings of this work are:

[39] 1. The averaging routine can significantly affect the calculated CO_2 fluxes. In this work in the North Atlantic differences of up to 47% were observed between calculation routines and the bias was more pronounced at higher fluxes. Using grid-averaged ΔpCO_2 and temperature appears appropriate, but grid-averaged wind speed data lead to biased results. The wind speed is a property that will change on much shorter spatiotemporal scales compared to the ΔpCO_2 and therefore the wind speed variance over the domain and time interval is needed.

[40] 2. This region of the North Atlantic represents a perennial sink for CO_2 and due to the lower wintertime pCO_2 sw, and the western sector displays a 46% greater sink than the eastern sector.

[41] 3. The choice of wind speed product introduces a small flux bias of around 4% with the NCEP/NCAR data product yielding a slightly lower flux than the QuikSCAT data.

[42] 4. The climatological CO_2 fluxes are similar to the observed values for the entire region. However, locally flux differences are more significant particularly in regions of the North Atlantic that are north of 45°N.

[43] **Acknowledgments.** We sincerely thank Wallenius Lines AS, Stockholm/Sweden, for cooperation and generous support. Furthermore, we are indebted to Yukihiro Nojiri for his pCO_2 system that was installed onboard the M/V *Falstaff*, Alexander Sy, who generously provided the thermosalinograph, Joaquin Triñanes for providing the QuikSCAT and NCEP/NCAR data, and Truls Johannessen and Are Olsen for very helpful comments. The authors also thank the Editor and two anonymous reviewers for their comments and suggestions, which helped to improve this work. This work was funded by the European Commission through the CAVASSOO project under grant EVK2-CT-2000-00088. This research was carried out in part under the auspices of the Cooperative Institute for Marine and Atmospheric Studies (CIMAS), a joint institute of the University of Miami and the National Oceanic and Atmospheric Administrative, cooperative agreement NA17RJ1226. The findings and conclusions in this report are those of the authors and do not necessarily represent the views of the funding agency.

References

Anderson, L. A., and A. Olsen (2002), Air-sea flux of anthropogenic carbon dioxide in the North Atlantic, *Geophys. Res. Lett.*, *29*(17), 1835, doi:10.1029/2002GL014820.

Chipman, D. W., J. Marra, and T. Takahashi (1993), Primary production at 47°N and 20°W in the North Atlantic Ocean: A comparison between the ^{14}C incubation method and mixed layer carbon budget observations, *Deep Sea Res., Part II*, *40*, 151–169.

Dickson, R., J. Lazier, J. Meincke, P. Rhines, and J. Swift (1996), Long-term coordinated changes in the convective activity of the North Atlantic, *Prog. Oceanogr.*, *38*, 241–295.

Doney, S. C. (1996), A synoptic atmospheric surface forcing data set and physical upper ocean model for the U.S. JGOFS Bermuda Atlantic Time Series Study (BATS) site, *J. Geophys. Res.*, *101*, 25,615–26,634.

Feely, R. A., R. Wanninkhof, H. B. Milburn, C. E. Cosca, M. Stapp, and P. Murphy (1998), A new automated underway system for making high precision pCO_2 measurements onboard research ships, *Anal. Chim. Acta*, *377*, 185–191.

Keeling, R. F., B. B. Stephens, R. Najjar, S. C. Doney, D. Archer, and M. Heimann (1998), Seasonal variations in the atmospheric O_2/N_2 ratio in relation to the kinetics of air-sea gas exchange, *Global Biogeochem. Cycles*, *12*(1), 141–163.

Lefèvre, N., A. J. Watson, D. J. Cooper, R. F. Weiss, T. Takahashi, and S. C. Sutherland (1999), Assessing the seasonality of the oceanic sink for CO_2 in the Northern Hemisphere, *Global Biogeochem. Cycles*, *13*(2), 273–286.

Lüger, H., D. W. R. Wallace, A. Körtzinger, and Y. Nojiri (2004), The pCO_2 variability in the midlatitude North Atlantic Ocean during a full annual cycle, *Global Biogeochem. Cycles*, *18*, GB3023, doi:10.1029/2003GB002200.

Meissner, T., D. Smith, and F. Wentz (2001), A 10–year intercomparison between collocated SSM/I oceanic surface wind speed retrievals and global analyses, *J. Geophys. Res.*, *106*, 11,719–11,729.

Olsen, A., A. Omar, A. C. Stuart-Menteth, and J. A. Triñanes (2004), Diurnal variations of surface ocean pCO_2 and sea-air CO_2 flux evaluated using remotely sensed data, *Geophys. Res. Lett.*, *31*, L20304, doi:10.1029/2004GL020583.

Olsen, A., R. Wanninkhof, J. A. Triñanes, and T. Johannessen (2005), The effect of wind speed products and wind speed-gas exchange relationships on interannual variability of the air-sea CO_2 gas transfer velocity, *Tellus, Ser. B*, *57*, 95–106.

Sweeney, C., T. Takahashi, A. Gnanadesikan, R. Wanninkhof, R. A. Feely, G. Friedrich, F. Chavez, N. R. Bates, J. Olafsson, and J. Sarmiento (2002), Spatial and temporal variability of surface water pCO_2 and sampling strategies, in *A Large-Scale CO2 Observing Plan: In Situ Oceans and Atmosphere (LSCOP)*, Appendix D, pp. 155–175, NOAA, Silver Spring, Md.

Takahashi, T., J. Olafsson, J. G. Goddard, D. W. Chipman, and S. C. Sutherland (1993), Seasonal variation of CO_2 and nutrients in the high-latitude surface oceans: A comparative study, *Global Biogeochem. Cycles*, *7*(4), 843–878.

Takahashi, T., et al. (2002), Global sea-air CO_2 flux based on climatological surface ocean pCO_2 and seasonal biological and temperature effects, *Deep Sea Res., Part II*, *49*, 1601–1622.

Völker, C., D. W. R. Wallace, and D. Wolf-Gladrow (2002), On the role of heat fluxes in the uptake of anthropogenic carbon in the North Atlantic, *Global Biogeochem. Cycles*, *16*(4), 1138, doi:10.1029/2002GB001897.

Wallace, D. W. R. (2002), Storage and transport of excess CO_2 in the oceans: The JGOFS/WOCE global CO_2 survey, in *Ocean Circulation and Climate*, edited by G. Siedler, J. Church, and J. Gould, pp. 489–521, Elsevier, New York.

Wanninkhof, R. (1992), Relationship between gas exchange and wind speed over the ocean, *J. Geophys. Res.*, *97*, 7373–7381.

Wanninkhof, R., S. C. Doney, T. Takahashi, and W. R. McGillis (2002), The effect of using time-averaged winds on regional air-sea CO_2 fluxes, in *Gas Transfer at Water Surfaces*, *Geophys. Monogr. Ser.*, edited by M. A. Donelan et al., vol. 127, edited by pp. 351–356, AGU, Washington, D. C.

Weiss, R. F. (1974), Carbon dioxide in water and seawater: The solubility of a non-ideal gas, *Mar. Chem.*, *2*, 203–215.

A. Körtzinger and D. W. R. Wallace, Leibniz-Institut für Meereswissenschaften and der Universität Kiel (IFM-GEOMAR), Kiel, Germany.

H. Lüger, Cooperative Institute of Marine and Atmospheric Sciences, Miami, FL, USA. (heike.lueger@noaa.gov)

R. Wanninkhof, Ocean Chemistry Division, Atlantic Oceanographic and Meteorological Laboratory, NOAA, Miami, FL, USA.